The stellar populations of nearby radiogalaxies

I. Aretxaga[1], E. Terlevich[1], R.J. Terlevich[2,1], G. Cotter[3], and A.I. Díaz[4]

[1] INAOE, Aptdo. Postal 51 y 216, Puebla, Pue., Mexico
[2] IoA, Univ. of Cambridge, UK
[3] Cavendish Lab., Univ. of Cambridge, UK.
[4] Dpto. Física Teórica, UAM, Spain.

Abstract. We present results on a sample of 7 nearby luminous radiogalaxies ($z < 0.08$, $P_{178\mathrm{MHz}} \gtrsim 10^{25}$ W Hz^{-1} Sr^{-1}), which mostly correspond to the FR II class. In two cases, Hydra A and 3C 285, the Balmer and λ4000 break indices constrain the spectral types and luminosity classes of the stars involved, revealing that the blue spectra are dominated by blue supergiant and/or giant stars. The ages derived for the last burst of star formation in Hydra A are between 7 and 40 Myr, and in 3C 285 about 10 Myr. The rest of the narrow-line radiogalaxies (four) have λ4000 break and metallic indices consistent with those of elliptical galaxies. The only broad-line radiogalaxy in our sample, 3C 382, has a strong featureless blue continuum and broad emission lines that dilute the underlying blue stellar spectra.

1 Introduction

In recent years direct evidence that star formation plays an important role in Active Galactic Nuclei (AGN) has been gathered [9][3][1][4] through the detection of stellar atmospheric features that indicate that most of the UV-NIR light coming from the nuclei of Seyfert 2 and LINERs is dominated by young starbursts. The evidence of these starbursts strongly supports some kind of Starburst-AGN connection. However, it is still to be demonstrated that starbursts play a key role in *all* kinds of AGN.

One of the most stringent tests *to assess if all AGN have associated enhanced nuclear star formation* is the case of lobe-dominated radio-sources, whose host galaxies have relatively red colours when compared to other AGN varieties. In this paper we address the stellar content associated with the active nuclei of a sample of FR II radiogalaxies, the most luminous class of radiogalaxies which possess the most powerful central engines and radio-jets [7]. The presence of extended collimated radio-jets, which fuel the extended radio structure over $\gtrsim 10^8$ yr, strongly suggests the existence of a supermassive accreting black hole in the nuclei of these radiogalaxies. This test addresses the question of whether AGN that involve conspicuous black holes and accretion processes also contain enhanced star formation.

2 Spectra and analysis

Our sample of radiogalaxies was extracted from the 3CRR catalogue [5] with the only selection criteria being edge-brightened morphology, which defines the

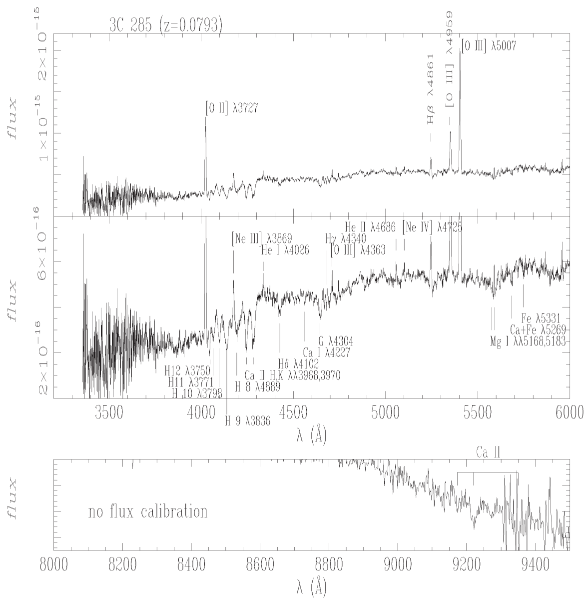

Fig. 1. Blue (top) and red (bottom) spectrum of 3C 285. The middle panels shows an enlargment of the continuum and absorption features of the blue-arm spectrum.

FR II class of radiogalaxies and redshift $z < 0.08$. Six out of a complete sample of ten FR II radiogalaxies that fulfill these requirements were randomly chosen. In addition to this sub-sample of FR IIs, we observed the unusually luminous FR I radiogalaxy Hydra A (3C 218). This has a radio luminosity which is an order of magnitude above the typical FR I/FR II dividing luminosity.

Spectroscopic observations of this sample were performed using the double-arm spectrograph ISIS mounted in the Cassegrain Focus of the 4.2m William Herschel Telescope in 1997 November 7–8 and 1998 February 19–20 (see Fig. 1).

2.1 Line and continuum measurements

The CaT index was detected in all of the objects, although in three cases (3C 285, 3C 382 and 4C 73.08) it was totally or partially affected by residuals left by the atmospheric band corrections and the measurement of its strength was thus precluded. For the remaining cases, the strength was measured in the rest-frame of the galaxies against a pseudo-continuum [9]. The values corrected for velocity dispersions (202 – 292 km/s) range between 6.2 and 7.0 Å.

Stellar populations can be dated through the measurement of the λ4000 or Balmer breaks. In intermediate to old populations the discontinuity at λ4000 results from a combination of the accumulation of the Balmer lines towards the limit of the Balmer absorption continuum at $\lambda3646$ (the Balmer break) and the increase in stellar opacity caused by metal lines shortwards of $\lambda4000$.

Table 1 lists the values of the $\lambda4000$ break index, $\Delta4000$Å, measured in the spectra of the 6 narrow-line radiogalaxies and the elliptical galaxy in our sample. This excludes 3C 382, which has a spectrum dominated by a strong blue continuum and broad-emission lines, and shows very weak stellar atmospheric features and no break. We adopted a definition [2] which quantifies the ratio of the average flux-level of two broad bands, one covering the break (3750-3950) and one bluewards of the break (4050-4250).

Hydra A and 3C 285 have spectra which are much bluer than those of normal elliptical galaxies. In order to quantify better the strength of the break and the ages of the populations derived, we have performed a bulge subtraction using as template the spectrum of NGC 4374, scaled to eliminate the G-band absorption of the radiogalaxies. Since the velocity dispersion of the stars in NGC 4374 and in the radiogalaxies are comparable inside the spectral resolution of our data, no further corrections were needed. The G-band absorption is prominent in stars of spectral types later than F5 and it is especially strong in types K. Thus, by removing a scaled template of NGC 4374, we are isolating the most massive stars ($M \gtrsim 1M_{\odot}$) in the composite stellar population of the radiogalaxies. Fig. 2 shows the bulge subtractions obtained on these two radiogalaxies.

We measured on the bulge-subtracted spectra $\Delta4000$Å and also the Balmer break index as defined by the classical $D\lambda_1$ method of stellar classification designed by Barbier and Chalonge [8]. The latter quantifies the Balmer discontinuity in terms of the logarithmic difference of the continuum levels (D) and the effective position of the break (λ_1). The method places a pseudo-continuum on top of the higher order terms of the Balmer series in order to measure the effective position of the discontinuity. The functional dependences on the effective temperature and gravity of the stars are sufficiently different for D and λ_1 to satisfy a two-dimensional classification.

The $D\lambda_1$ method could only be reliably applied in the cases of Hydra A and 3C 285. For the other radiogalaxies, the bulge-subtractions led to results that did not allow the identification of the absorption features and/or the break in an unambiguous way due to the resulting poor S/N.

Table 1 lists the $\lambda4000$ and Balmer break indices measured in both the bulge-subtracted and the original spectra of the radiogalaxies.

3 Discussion

3.1 Comparison with elliptical galaxies and population synthesis models

The radiogalaxies 3C 98, 3C 192, 4C 73.08 and DA 240 have indices of the order of 1.9 to 2.3, which overlap with those of normal E galaxies, $\Delta4000\text{Å} = 2.08 \pm 0.23$. These values correspond to populations dominated by stars of ages 1 to 10 Gyr old, if one assumes coeval population synthesis models[6].

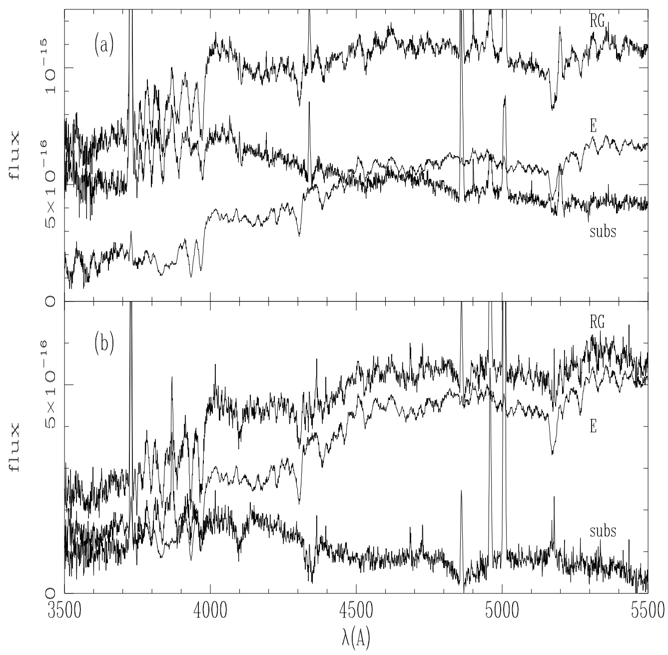

Fig. 2. Bulge-subtraction for (a) Hydra A and (b) 3C 285. We show the original spectra of the radiogalaxy (RG), the scaled template spectra of the bulge population (E), and the resulting bulge-subtracted spectra (subs).

Table 1. Break indices

object	original spectra Δ4000Å mag	bulge-subtracted spectra Δ4000Å mag	D	λ_1 Å
3C 98	2.1			
3C 192	1.9			
Hydra A	1.4	1.2	0.26–0.28	3746–3752
3C 285	1.6	1.0	0.48–0.53	3740–3746
4C 73.08	2.2			
DA 240	2.2			
NGC 4374	2.3			

However, Hydra A and 3C 285 have indices in the range 1.4 to 1.6, typical of coeval populations which are 200 to 500 Myr old. Once the bulge population is subtracted, the Δ4000Å indices of Hydra A and 3C 285 decrease to 1.2 and 1.0 respectively, which are typical of systems younger than about 60 Myr.

Hamilton (1985) measured the Δ4000Å index in a sample of stars covering a wide range of spectral types and luminosity classes. He found a sequence of increasing Δ4000Å from B0 to M5 stars, with values from 1 to 4 mag respectively. A comparison with the sequence he found leads us to conclude that the break in the bulge subtracted spectrum of Hydra A is dominated by B or earlier type stars while that of 3C 285 is dominated by A type stars. The index Δ4000Å does not clearly discriminate luminosity classes for stars with spectral types earlier than G0.

The equivalent width of the H10 absorption line in these two radiogalaxies give further support to the interpretation of the Balmer break as produced by a young stellar population. In Hydra A we find after bulge subtraction EW(H10)$\approx$ 3.9Å, which, according to the synthesis models of González-Delgado et al. (2000) gives ages of 7 to 15 Myr for an instantaneous burst of star formation, and 40 to 60 Myr for a continuous star formation mode, in solar metallicity environments. In the case of 3C 285, EW(H10)$\approx$ 6Å would imply an age older than about 25 Myr for a single-population burst of solar metallicity.

The metallic indices of normal elliptical galaxies range between the values $0.56 \log[\mathrm{MgFe}] 0.66$ (González 1993), which characterizes oversolar metallicites for ages larger than about 5 Gyr. This is also the typical range of our radiogalaxies, although 3C 285 shows a clear departure with $\log[\mathrm{MgFe}] \approx 0.4$. However, [MgFe] tends to be smaller for populations younger than a few Gyr and similar oversolar metallic content. Since 3C 285 has a clear burst of recent starformation, we conclude that its overall abundance is also most probably solar or oversolar.

3.2 The blue stellar content

A better estimate of the spectral type and luminosity class of the stars that dominate the break in Hydra A and 3C 285 comes from the two-dimensional classification of Barbier and Chalonge. In Figure 8 the solid squares connected by lines represent the maximum range of possible $D\lambda_1$ values measured in these radiogalaxies.

The Balmer break index is sensitive to the positioning of the pseudo-continuum on top of the higher order Balmer series lines, which in turn is sensitive to the merging of the wings of the lines, enhanced at large velocity dispersions. In order to assign spectral types and luminosity classes to the stars that dominate the break, therefore, it is not sufficient to compare the values we have obtained with those measured in stellar catalogues. The values measured for the radiogalaxies can be corrected for their intrinsic velocity dispersions; we have chosen instead to recalibrate the index using template stars of different spectral types and luminosity classes convolved with gaussian functions, until they reproduce the width of the Balmer lines observed in the radiogalaxies (FWHM$\approx$ 12.5Å). We used the B0 to A7 stars from the stellar library of Jacoby et al. (1984), which were observed with 4.5Å resolution. The values of the $D\lambda_1$ indices measured in these broadened stars are represented in Figure 8 by their respective classification. By comparison we also plot the grid traced by the locus of unbroadened stars, as published by Strömgren (1963). The broadening of the lines shifts the original locus of supergiant stars from the $\lambda_1 3720$Å range (Chalonge 1956) to the $3720\lambda_1 3740$Å range, occupied by giant stars in the original (unbroadened) classification. Giant stars, in turn, shift to positions first occupied by dwarfs. Most dwarfs have Balmer line widths comparable to those of the radiogalaxies, and thus their locus in the diagram is mostly unchanged.

The value of the D index indicates that the recent burst in Hydra A is dominated by B3 to B5 stars, and the effective position of the Balmer break (λ_1) indicates that these are giant or supergiant stars, respectively. These stars have masses of 7 and $20 M_\odot$ (Schmidt-Kaler 1982). From the stellar evolutionary tracks of massive stars with standard mass-loss rate at or 2 (Schaller et al. 1992, Schaerer et al. 1993, Meynet et al. 1994) we infer that these stars must have ages between 7 to 8 Myr (B3I) and 40 Myr (B5III). Note that the B4V stars in Figure 8, near the location of Hydra A, cannot originate the break and at the same time follow the kinematics of the nucleus (see section 5.3). Any dwarf star located in the stellar disk of Hydra A would show absorption lines that have been broadened beyond the 12.5Å of FWHM we measure in this radiogalaxy, and its position would have been shifted further into larger values of λ_1.

The location in the $D - \lambda_1$ plane of 3C 285 indicates that the break is produced by A2I stars. These are $15 M_\odot$ stars. Again, ages of 10 to 12 Myr are found for the last burst of star formation in this radiogalaxy. The interpretation of the blue excess in terms of A type stars is further supported by the detection of the Ca II H line in the bulge-subtracted spectrum.

3.3 The red stellar content

The CaT index in the radiogalaxies has values between 6 and 7Å. Díaz et al. (1989) find that at solar or oversolar metallicities red supergiant stars have CaT indices ranging from 8.5 to 13Å, red giant stars from 6 to 9Å and dwarfs from 4.5 to 8.5Å. The values we find are thus compatible with both giant or dwarf stars. However, we favour the interpretation of giant stars since the old bulge population will be dominated by red giants, as in the case of elliptical galaxies.

We have measured the CaT in a control sample of elliptical galaxies observed by J. Gorgas and collaborators (priv. communication) and combined these measurements with those found by Terlevich et al (1990) in a sample of elliptical, lenticular, spiral, and active galaxies of different kinds. We find that the range of CaT in elliptical galaxies, 5 to 7.5Å, comprises the range of values of the radiogalaxies (see Figure 9).

García-Vargas, Mollá & Bressan (1998) find in their population synthesis models values of the CaT between 6 and 7Å for ages ranging from 100 Myr to 1 Gyr, and larger afterwards, assuming coeval star formation and solar or oversolar metallicity. A revised version of these models by Mollá & García-Vargas (2000) which includes extended libraries of M-type stars, predicts for ages between 2 and 20 Gyr a constant value of 7Å at solar metallicity, and 8.5Å at 2. These synthesis models are based on parametric fittings of the CaT strength in NLTE model atmospheres (Jørgensen, Carlsson & Johnson 1992) and in fittings of empirical values measured in stellar libraries (e.g. Díaz et al. 1989; Zhou 1991). The fits work well in the low metallicity regime. However, at metallicities higher than solar, the relationship between metallicity and the CaT index shows a big scatter, and the linear fittings loose any predictive power (see Figure 4 of Díaz et al. 1989).

Red supergiant stars appear in coeval population synthesis models between 5 and 30 Myr, and create a maximum strength of the CaT index (CaT $\gtrsim$ 9Å) around 6 to 16 Myr for and 5 to 30 Myr for 2 (García-Vargas et al. 1993, 1998; Mayya 1997). Strengths of CaT $\gtrsim$ 7Å are characteristic of bursts with ages between 5 and 40 Myr. Leitherer et al. (1999) also find that the total strength of the population depends dramatically on the slope of the initial mass function (IMF) and star formation history. While a coeval burst with a complete Salpeter IMF yields values surpassing 7Å between 6 and 12 Myr, the same IMF in a continuous star formation mode yields values of only 5.5Å maximum. The CaT strength values for coeval star formation derived by Leitherer et al. (1999) differ substantially from those derived by García-Vargas and coworkers (1993, 1998) and by Mayya (1997), most probably due to a different calibration of the CaT index.

Mixed populations of young bursts which contain red supergiants, superposed on old populations can also yield values of the CaT between 4 and 8Å (García-Vargas et al. 1998). Since metal rich giant stars have CaT values ranging from 6 to 9Å we regard our observations of the CaT index in radiogalaxies, as being compatible with ages 1 to 15 Gyr.

References

1. González Delgado R. M. et al.: 1998, ApJ, 505, 174
2. Hamilton D.: 1985, ApJ, 297, 371.
3. Heckman T.M. et al.: 1997, ApJ, 482, 114.
4. Kunth D., Contini T.: 1999, in IAU Symp. 193 *'Wolf-Rayet Phenomena in Massive Stars and Starburst Galaxies'*, eds. K.A. van der Hucht et al., ASP, p. 725.
5. Laing R.A., Riley J.M., & Longair M.S.: 1983, MNRAS, 204, 151.
6. Longhetti M., Bressan A., Chiosi C., Rampazzo R.: 1999, AA, 345, 419.
7. Rawlings S., Saunders R.: 1991, Nat., 349, 138.
8. Strömgren B., in 'Basic Astronomical Data, Stars and Stellar Systems', vol. 3, p. 123.
9. Terlevich E., Díaz A.I., Terlevich R.: 1990, MNRAS, 242, 285.